Either a permanent or a programmable transmission filter element can be employed. For a given emission source, a flame for example, the spectra are not dynamic in that they do not change on a measurement-to-measurement basis. If the source temperature remains relatively constant, there is no need to change the filter function. Thus, a permanent transmission mask may be employed. Permanent transmission filter masks can be produced by several methods. One method is to use the emission and background spectra of the species to be analyzed as a basis set. This basis set is then orthogonalized using a digital computer. The resulting basis set and the factorization matrix (5) may then be used to produce enlarged dot density masks on a digital plotter. These enlarged masks could then be photographically reduced to proper dimensions. If programmability is required, for example in cases where the interferences vary substantially over time, then a liquid crystal device such as the ones found in the new "pocket" television sets could be used for the transmission mask.

Promising applications are those that apply the optical correlation filter method to spectroscopic analyses which are background emission interference limited. One example is the detection of alkali and alkali earth elements by flame emission. Interferences due to the combustion products of the fuel and due to emission from other species in the sample will limit the detection. Another application will be found in ICP emission for quantitative estimation of atomic species. It is well-known that interference, as a consequence of the great number of emission lines relative to that of absorption, is a limiting factor in emission spectroscopies. In this case several correlation filter functions would be constructed such that they would be orthogonal to each other.

The main advantage to incoherent OSP is that the optical spectrum or interferogram can be processed without conversion. By use of achromatic transmission elements, the processor will be unaffected by the chromaticity of the signal. Another advantage is in the short time required to "calculate" the signal estimate. OSP can perform parallel computations in the same time that is required to perform one computation. Thus, entire spectral libraries may be "searched" in one operation. A third advantage is that the data are already in a form that can be utilized by the processor. Only minor electronic level computations are required for the mathematical formulation of the signal estimate. Fourth, the cost of an optical processor can be much less than a large digital array processor. And finally, the physical size of the optical processor will allow construction of spectrometers that contain all of the processing capabilities. It should not be difficult to add this processor to existing dispersion devices, since the only additional components required are transmission filters and photodiodes.

One disadvantage is that the throughput of the signal may be low when there is a large overlap between target spectra and interference spectra (2, 3). This is especially true if there is a large number of such interferences. The optical correlation filter transmission element will have a maximum total spectrum throughput on the order of the integrated spectral density and half of this per photodiode for two (bipolar) correlation filter vectors. The more elements in a matched filter "library", the less total light throughput per element, scaling at best as $1/2N$, N being the number of filter elements. However, the correlation filter maximizes the signal-to-noise ratio, and the throughput at wavelengths that are correlated to a particular spectrum should approach 100%. For large numbers of correlation filter elements in a single mask element, the spectroscopic signal may be amplified with a image intensifier. Alternatively, the correlation filter can be time multiplexed in the spectral image plane so that only one pattern is correlated at a time (1).

CONCLUSION

The application of OSP to spectroscopic-based chemical analysis problems will result in more efficient means to both obtain signal estimates that are independent of background interferences and to perform rapid pattern recognition spectral analysis. Further, the OSP spectroscopic data analyzer will be a cost-effective alternative to processing of fast analytical signals. Specific applications of the OSP spectrum processor will be found for the real-time discrimination and quantitative estimation of luminescent spectroscopic signals that are background limited.

A surprisingly straightforward application of optical signal processing to a particular class of problems currently limiting several analysis processes has been described here. This device could prove to make light work out of what with current technology requires large amounts of computer time, labor, and/or expensive analysis equipment. The device will be very well suited for use as a chemical sensor, which will respond to only the species of interest. This sensor would not have to be large in size and could be constructed from materials currently available.

LITERATURE CITED

(1) Rhodes, W. T.; Sawchuk, A. A. In *Optical Signal Processing Fundementals*; Lee, S. H., Ed.; Springer-Verlag: New York, 1981.
(2) Morgan, D. R. *Appl. Spectrosc.* **1978**, *31*, 404–414; 1978, *31*, 415–423.
(3) Morgan, D. R. *General Electric Technical Report* R75ELS024, 1975.
(4) Papoulis, A. *Probability, Random Variables and Stochastic Processes*, 2nd ed.; McGraw-Hill: New York, 1984.
(5) Golub, G. H.; Van Loan, C. F. *Matrix Computations*; Johns Hopkins University Press: Baltimore, MD, 1983.
(6) Bialkowski, S. E. *Anal. Chem.* **1986**, *58*, 1706–1710.
(7) Casasent, D.; Jackson, J.; Neuman, C. P. *Appl. Opt.* **1983**, *22*, 115–124.
(8) Casasent, D. *Proc. IEEE* **1984**, *72*, 831–849.

Stephen E. Bialkowski
Department of Chemistry and Biochemistry
Utah State University
Logan, Utah 84322–0300

RECEIVED for review March 18, 1986. Accepted June 19, 1986. Support for this work and other projects from the Office of the Vice President for Research at Utah State University is gratefully acknowledged.

Sequencing Procyanidin Oligomers by Fast Atom Bombardment Mass Spectrometry

Sir: Polymeric procyanidins (condensed tannins) are present in a wide distribution of plants, occurring in particularly high concentrations in some barks, leaves, and fruits (1). These phenolic polymers complex with proteins and therefore inhibit enzyme activity (2), are important contributors to the flavor of foods (3, 4), and influence the nutritional value of plants (5, 6). Procyanidins are also credited with a role in protecting plants from microorganisms and insects (7,

0003-2700/86/0358-2563$01.50/0 © 1986 American Chemical Society

8). As abundant constituents of the barks of many commercially harvested timber species, procyanidins are potential replacements for petroleum-derived, phenolic polymers used industrially as adhesives, dispersants, and ion exchange materials (9–11). Although these polymers have been used throughout recorded history in applications such as leather tanning (12), little was known about their chemistry until recently. Current research is for the most part focused on their biogenesis, structure, and reactions (13–19).

Both ^{1}H and ^{13}C NMR spectroscopy have been primary tools for elucidating procyanidin structures. However, resonance multiplicity and broadening associated with rotational and conformational isomerism often severely complicate the interpretation of NMR spectra. Although remarkable advances have been made in elucidating the structures of these polymers over the past 15 years, questions remain about the occurrence and extent of branching, the relative proportions of different interflavanoid linkage types, and the sequential order of different monomer units in the polymers.

A growing body of literature (20, 21) advocates the use of fast atom bombardment mass spectrometry (FAB-MS) coupled with some mode of tandem mass spectrometry (MS–MS) (22, 23) as a powerful tool for partial or complete sequencing of biopolymers. This correspondence describes the sequencing of procyanidin oligomers by FAB-MS and linked scanning MS–MS. The abundant sequence ions observed can also be used to differentiate the two types of polymeric linkages found in procyanidins as well as to distinguish a branched trimer from linear isomers. Metastable decomposition pathways leading to the sequence ions are established for each compound.

EXPERIMENTAL SECTION

Procyanidin dimer A-1, epicatechin(4β→8;2β→O→7)catechin (I), was isolated from Arachis *hypogea* (24). The dimeric procyanidins B-1, epicatechin(4β→8)catechin (II), and B-7, epicatechin(4β→6)catechin (III), were made by acid-catalyzed cleavage of condensed tannins isolated from *Pinus taeda* bark in the presence of excess (+)-catechin (16). The branched trimer epicatechin(4β→8)catechin(4β→6)epicatechin (IV) was synthesized by reacting III with epicatechin-4β-phenyl sulfide at pH 9.0 and ambient temperature (15, 17). The linear trimers epicatechin(4β→8)epicatechin(4β→6)catechin (V) and epicatechin-(4β→8)epicatechin(4β→8)catechin (VI) were isolated from the phloem of *Pinus taeda* (25).

Mass spectra were obtained with a VG 7070E-HF mass spectrometer. A standard VG FAB source equipped with an Ion Tech saddle field atom gun was used. The sample compounds were dissolved in droplets of the FAB liquid matrix, a 5:1 mixture of dithiothreitol and dithioerythritol, directly on the target of the sample insertion probe. The samples were bombarded with 8 keV xenon atoms; the resulting secondary ions were accelerated from the source to 6 keV and mass analyzed at low resolution (1500–2000, 10% valley definition) with a scan rate of 10 s per mass decade. Metastable decomposition pathways were established with B/E and B^2/E linked scanning without collisional activation.

RESULTS AND DISCUSSION

The positive ion mass spectra produced by FAB-MS of the procyanidin oligomers (I–VI) all exhibit abundant $(M + H)^+$ ions; fragmentation occurs predominantly by cleavage of interflavanoid bonds to produce sequence ions. Retro-Diels–Alder (RDA) fission of the flavanoid monomer's heterocyclic ring system, similar to that recently reported for several flavonols (26), is also observed but to a lesser degree than the bond cleavages.

The dimers I, II, and III represent the two types of interflavanoid bonds found in procyanidins: the A-type (C4→C8;2β→O→7) double linkage as shown in the dimer A-1 (I) and the B-type (C4→C8 or C4→C6) carbon-to-carbon linkage as shown in dimers B-1 (II) and B-7 (III), respectively.

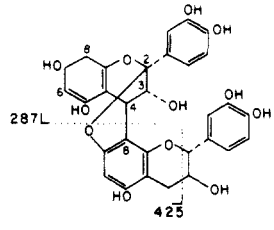

I

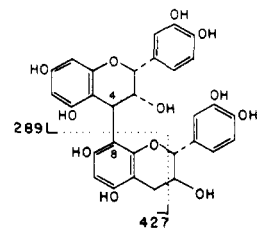

II

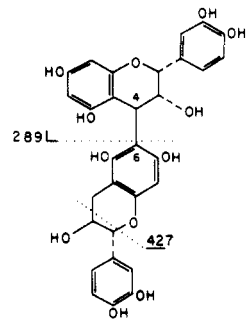

III

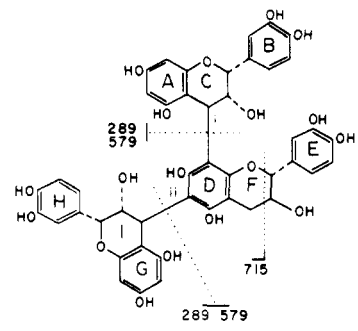

IV

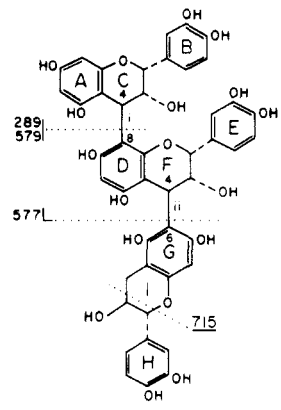

V

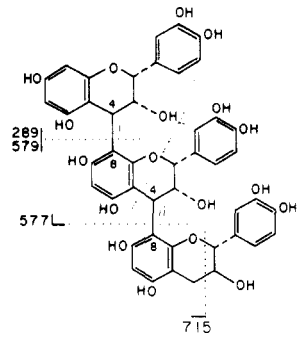

VI

Mass peaks corresponding to $(M + H)^+$ and $(M - H_2O + H)^+$ ions for I and III are observed at m/z 577/559 and 579/561, respectively (Figure 1); fragmentation characteristic of the interflavanoid bonds is readily apparent in the major ion peaks at m/z 287 for I and 289 for III. The spectrum of II, not shown, is qualitatively similar to that of III; the slight differences in relative abundances observed between corresponding peaks in the mass spectra of II and III are probably due to the different locations of their interflavanoid bonds. Ion peaks attributable to RDA fission and subsequent water loss are observed at m/z 425 and 407 for I and m/z 427 and 409 for II and III.

It is well documented that B-type procyanidin linkages, which readily undergo acid-catalyzed cleavage to give carbonium ions at the C4 position of the upper flavanoid unit (1, 27), are very acid labile in solution and that A-type linkages, which resist acid-catalyzed cleavage (24, 28), are not. Gas-phase decompositions of FAB-desorbed ions are known to mimic reactions in solution (20, 21); this is indeed the case with the two types of procyanidin dimers. Linked-scan spectra from $(M + H)^+$ and its principal daughter ions show that both m/z 287 from I and m/z 289 from II and III can result from gas-phase, unimolecular decompositions of the parent ions. However, in parallel to the reactions in solution chemistry, the metastable decomposition pathways leading to characteristic sequence ions from the dimers are distinctly different

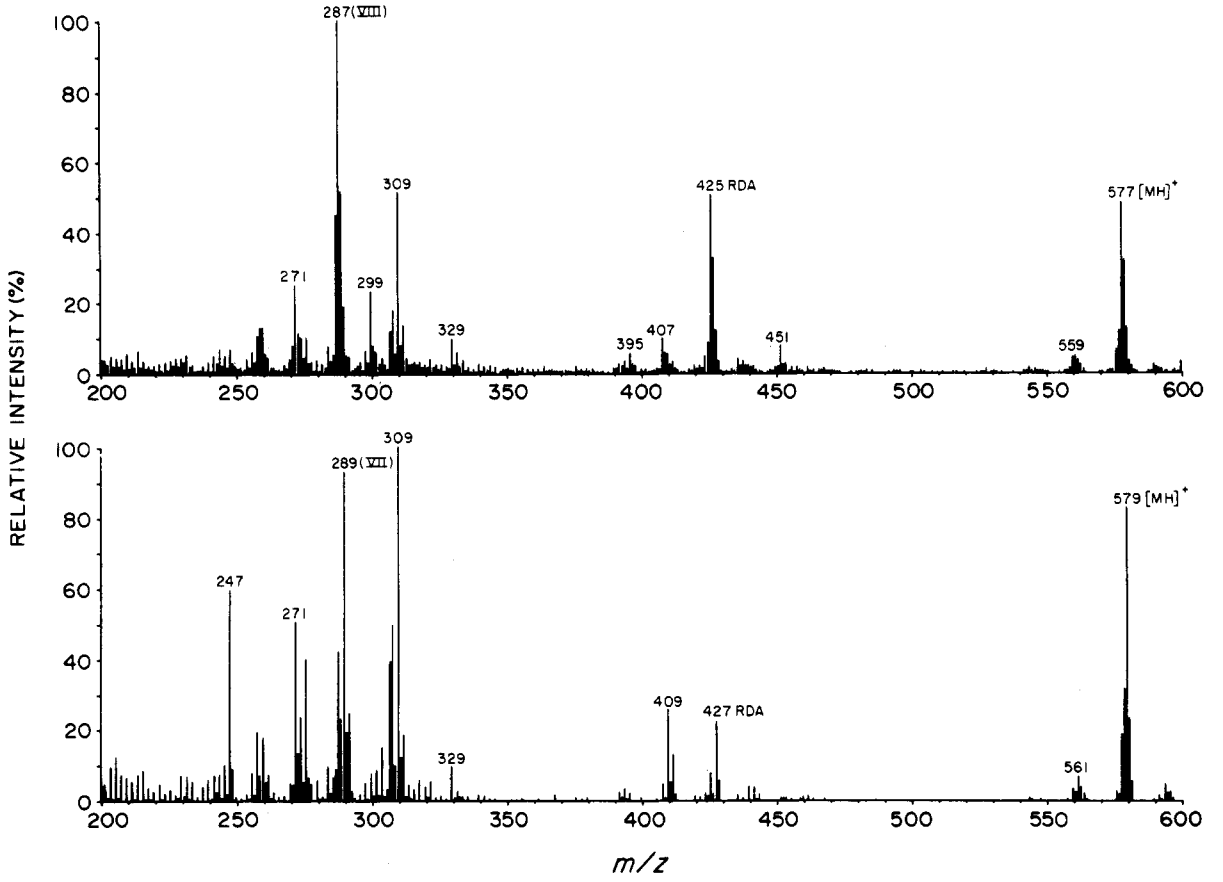

Figure 1. FAB mass spectra of procyanidin dimers (m/z 309 is a matrix ion peak): A-1 (I), upper spectrum; B-7 (III), lower spectrum.

for the two types of interflavanoid bonds (Figure 2A). In the case of B-type dimers, II and III, both B/E and B^2/E linked scans clearly show that the monomer ion at m/z 289 forms directly from the $(M + H)^+$ ion; the process can be pictured as simple protonation of the aromatic ring at the bonding carbon (C8 or C6) followed by bond cleavage to give the carbonium ion. By contrast, the A-1 dimer undergoes a two-step decomposition: RDA fission of the protonated parent ion, $(M + H)^+$, gives the ion at m/z 425, which subsequently decomposes to the monomer ion, m/z 287 (VIII).

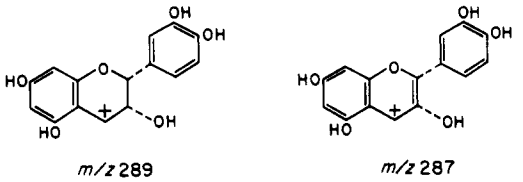

m/z 289 VII

m/z 287 VIII

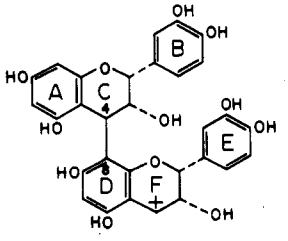

m/z 577 IX

The trimers IV–VI all give $(M + H)^+$ ion peaks at m/z 867 (Figure 3). Fragmentation of the upper interflavanoid linkage, i, in each leads to ion peaks at m/z 289 and 579. As in the case of the B-type dimers (II and III), the m/z 289 peak corresponds to the upper flavanoid unit, which can form a carbonium ion at C4 upon bond cleavage (VII). The m/z 579 ion peak corresponds to a protonated dimer moiety from the lower two flavanoid units.

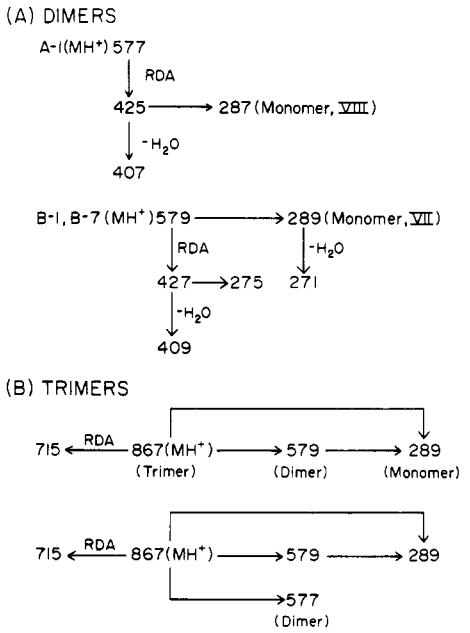

Figure 2. Metastable decomposition pathways leading to major sequence ions for procyanidin (A) dimers [A-1 (I), upper; B-1 and B-7 (II and III), lower] and (B) trimers [branched trimers (IV), upper; linear trimers (V and VI), lower].

However, fragmentation of the lower interflavanoid bond, ii, in the three trimers leads to different sequence ions depending on whether the trimer is branched or linear. In the

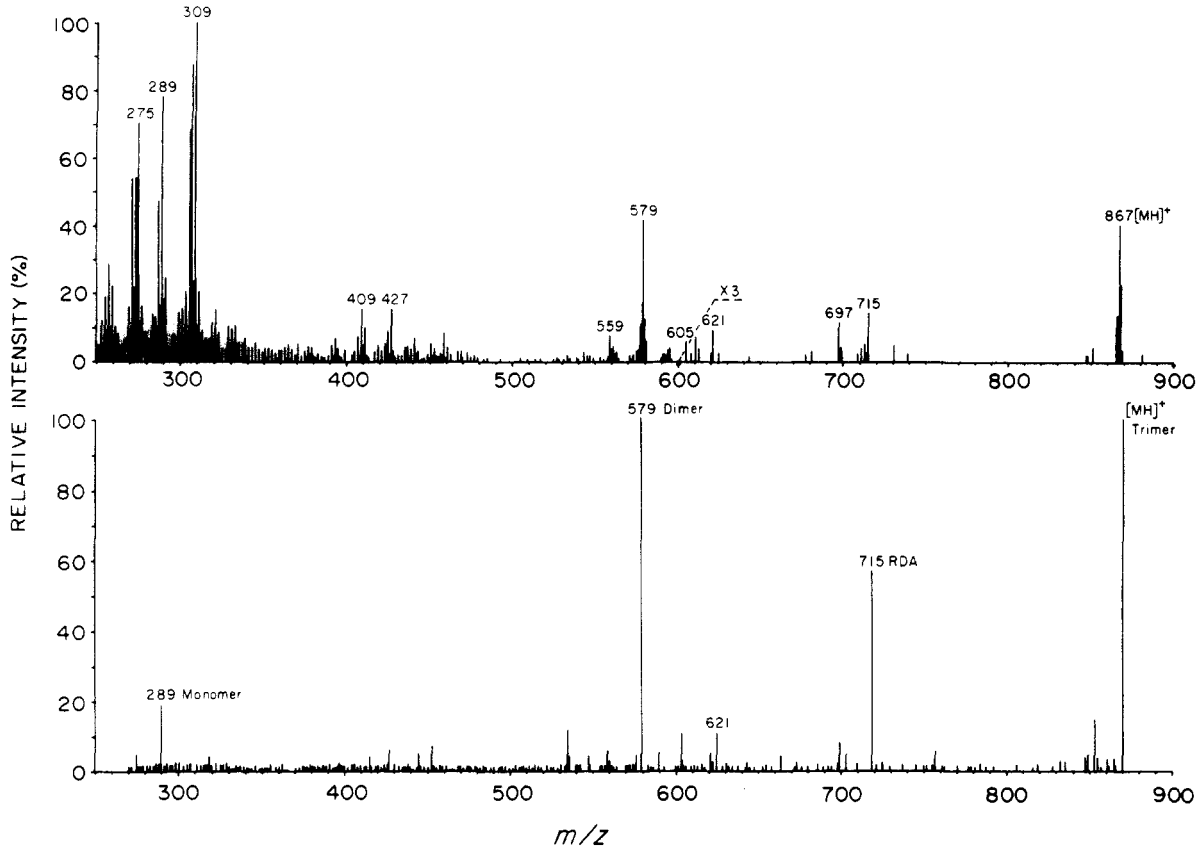

Figure 3. FAB mass spectrum of branched procyanidin trimer (IV) showing sequence ions at m/z 289 and 579 (upper spectrum); daughter ion linked scan showing unimolecular gas phase decomposition of $(M + H)^+$ ion (m/z 867) from (IV) above (lower spectrum).

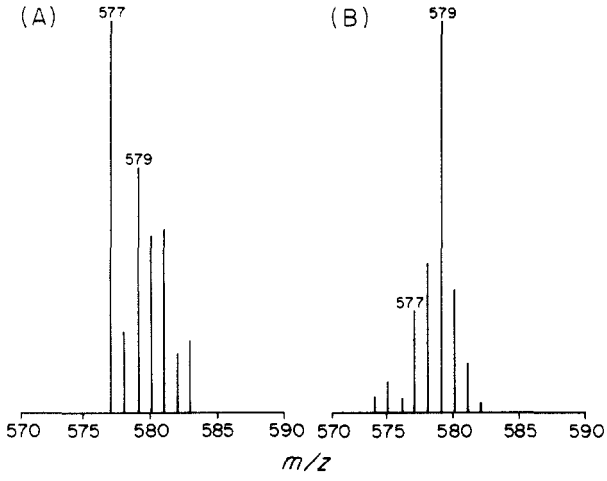

Figure 4. Dimeric regions of the mass spectra of (A) a linear trimer (V) and (B) a branched trimer (IV).

branched trimer (IV), cleavage of bond ii can only lead to formation of a carbonium ion at C4 of ring I, which again results in an ion peak at m/z 289 (VII). The upper two flavanoid units released on cleavage of bond ii give an ion peak at m/z 579 corresponding to a protonated dimer. Thus, in the spectrum of the branched trimer (Figure 3), sequence ions are observed only at m/z 289 and 579. B/E linked-scan spectra show that both sequence ions, in addition to the RDA fragment at m/z 715, can occur directly from unimolecular gas phase decomposition of $(M + H)^+$. By contrast, cleavage of the linear trimers (V and VI) at the lower bond, ii, gives a carbonium ion at C4 of the middle flavanoid unit (ring F), which results in formation of a dimer moiety with m/z 577 (IX). Thus, sequence ions observed for linear trimers occur at m/z 289, 577, and 579. Portions of typical mass spectra containing the dimer fragments of a linear and a branched trimer are compared in Figure 4. Figure 2B illustrates the metastable decomposition pathways leading to sequence ions for the branched (IV) and linear (V and VI) trimers.

The above findings show that procyanidin oligomers can be sequenced by FAB-MS, that information can be obtained about the type and location of the interflavanoid bonds, and that linear and branched oligomers can be differentiated on the basis of their fragmentation products. This information complements that which can be obtained by ^1H and ^{13}C NMR spectroscopy and forms a basis for structural elucidation of higher molecular weight polymers.

All of the experiments conducted in this study were performed on chromatographically isolated and purified samples; however, it should be feasible to extend the use of FAB coupled with MS–MS to the direct analysis of procyanidin oligomers without recourse to chromatographic isolation of pure compounds. The potential of this powerful approach to mixture analysis has already been demonstrated on a number of biopolymer systems (*20*, *21*) and should be equally applicable to the sequencing of procyanidin polymers. This possibility is currently being investigated.

Registry No. I, 103751-05-9; II, 20315-25-7; III, 103732-18-9; IV, 103751-06-0; V, 79763-28-3; VI, 79813-67-5.

LITERATURE CITED

(1) Haslam, E. In *The Flavonoids: Advances in Research*; Harborne, J. B., Marby, T. J., Eds.; Chapman and Hall: London, 1982; pp 417–447.
(2) Brown, B. R.; Lisseter, S. G. *Phytochemistry*, in press.
(3) Haslam, E. *Phytochemistry* **1977**, *16*, 1625–1640.
(4) Delcour, J. A.; Vandenberghe, M. M.; Dondeyne, P.; Schrevens, E. L.; Wijnhoven, J.; Moerman, E. *J. Inst. Brew.* **1984**, *90*, 67–72.
(5) Kumar, R.; Singh, M. *J. Agric. Food Chem.* **1984**, *32*, 447–453.
(6) Butler, L. G.; Riedl, D. J.; Lebryk, D. G.; Blytt, H. J. *J. Am. Oil Chem. Soc.* **1984**, *61*, 916–920.
(7) Klocke, J. A.; Chan, B. C. *J. Insect Physiol.* **1982**, *28*, 911–915.
(8) Zucker, W. V. *Am. Nat.* **1983**, *121*, 335–365.
(9) Hemingway, R. W. In *Organic Chemicals from Biomass*; Goldstein, I. S., Ed.; CRC Press: Boca Raton, FL, 1980; pp 189–248.
(10) Pizzi, A. In *Wood Adhesives, Chemistry and Technology*; Pizzi, A., Ed.; Marcel Dekker: New York, 1983; pp 177–246.

(11) Hemingway, R. W.; Laks, P. E.; McGraw, G. W.; Kreibich, R. E. In *Proceedings IUFRO Conference, Forest Products Research International—Achievements and the Future*; Pretoria, South Africa, 1985; Vol. 17, pp 1-20.
(12) Howes, F. N. *Vegetables Tanning Materials*; Butterworths: London, 1953; pp 152-156.
(13) Stafford, H. A.; Lester, H. H.; Porter, L. J. *Phytochemistry* **1985**, *24*, 333-338.
(14) Hemingway, R. W.; Laks, P. E. *J. Chem. Soc., Chem. Commun.* **1985**, 746-747.
(15) Foo, L. Y.; Hemingway, R. W. *J. Chem. Soc., Chem. Commun.* **1984**, 85-86.
(16) Hemingway, R. W.; Karchesy, J. J.; McGraw, G. W.; Wielsek, R. A. *Phytochemistry* **1983**, *22*, 275-281.
(17) Hemingway, R. W.; Foo, L. Y. *J. Chem. Soc., Chem. Commun.* **1983**, 1035-1036.
(18) Nonaka, G.; Morimoto, S.; Nishioka, T. *J. Chem. Soc., Perkin Trans. 1* **1983**, 2139-2145.
(19) Porter, L. J.; Newman, R. H.; Foo, L. Y.; Wong, H.; Hemingway, R. W. *J. Chem. Soc., Perkin Trans. 1* **1982**, 1217-1221.
(20) *Tandem Mass Spectrometry*; McLafferty, F. W., Ed. Wiley-Interscience: New York, 1983.
(21) *Mass Spectrometry in the Health and Life Sciences*; Burlingame, A. L.; Castagnoli, N., Jr., Eds.; Elsevier: New York, 1985; Chapters 9, 10, 12-14.
(22) McLafferty, F. W.; Bockhoff, F. M. *Anal. Chem.* **1978**, *50*, 69-76.
(23) Haddon, W. F. In *High Performance Mass Spectrometry*; Gross, M. L., Ed.; American Chemical Society: Washington, DC, 1978; pp 97-119.
(24) Karchesy, J. J.; Hemingway, R. W. *J. Agric. Food Chem.*, in press.
(25) Hemingway, R. W.; Foo, L. Y.; Porter, L. J. *J. Chem. Soc., Perkin Trans. 1* **1982**, 1209-1216.
(26) de Koster, C. G.; Heerma, W.; Dijkstra, G.; Niemann, G. J. *Biomed. Mass Spectrom.* **1985**, *12*, 596-601.
(27) Thompson, R. S.; Jacques, D.; Haslam, E.; Tanner, R. J. N. *J. Chem. Soc., Perkin Trans. 1* **1972**, 1387-1399.
(28) Jacques, D.; Haslam, E.; Bedford, G. R.; Greatbanks, D. *J. Chem. Soc., Perkin Trans. 1* **1974**, 2663-2671.

Joseph J. Karchesy*
Department of Forest Products
Oregon State University
Corvallis, Oregon 97331

Richard W. Hemingway
Southern Forest Experiment Station
Pineville, Louisiana 71360

Yeap L. Foo
Chemistry Division, DSIR
Petone, New Zealand

Elisabeth Barofsky
Douglas F. Barofsky
Department of Agricultural Chemistry
Oregon State University
Corvallis, Oregon 97331

RECEIVED for review December 26, 1985. Resubmitted June 9, 1986. Accepted June 9, 1986.. This is paper 2040, Forest Research Laboratory, Oregon State University, Corvallis, OR 97331. Support from USDA Grant 85-CRSR-2-2555 is gratefully acknowledged (J.J.K.).

Statistical Sampling Errors as Intrinsic Limits on Detection in Dilute Solutions

Sir: Sensitive detection schemes such as laser-induced fluorescence have reached levels of performance where single atoms can now be detected in the gas phase (*1*), and after complexation with fluorescein-labeled antibodies, single polymer chains have been detected on the surface of a microscope slide (*2*).

Failure to detect single molecules in a liquid phase has been ascribed to large background signals (*3*). Impressive reductions in background signals from Raman scattering (*4*) and window fluorescence (*5-7*) have now been achieved. Dovichi et al. (*3*) have predicted that single molecules could be detected in solution with reasonable improvements to laser flow cytometer detectors (*3*, *8*, *9*).

It is the purpose of this work to show that statistical sampling theory predicts poor precision for sampling microvolumes of very dilute solutions and presents an ultimate lower limit on detection. It will be shown that solvent molecules play a key role in setting this statistical limit, in contrast to gas and solid phase detection where a solvent is not required.

Sampling theory for chemical analysis (*10*) and in chemometrics (*11*, *12*) has been well-reviewed in the literature.

Sampling theory (*13*, *14*) can be applied to a simplified model of a homogenous solution. Consider a binary system consisting only of analyte and solvent. A binomial distribution predicts an analyte relative standard deviation for any binary system as

$$\sigma_A/n_A = ((1 - p)/n_T p)^{1/2} \quad (1)$$

where n_A is the number of analyte particles in the sample, σ_A is its standard deviation (heterogeneity between samples), n_T is the total number of particles in the sample, including solvent particles, and p is defined as

$$p = n_A/n_T \quad (2)$$

and $(1 - p)$ is then the corresponding fraction for solvent particles.

At concentrations typical of analysis, the solvent particles in liquid solutions far outnumber the analyte particles, and thus p is very small. At the same time, n_T is very large due to dense packing in liquids, even in the smallest possible volume. Equation 1 can now be simplified by the above conditions to give

$$\sigma_A/n_A = n_A^{-1/2} \quad (3)$$

Readers will recognize this result as the Poisson limit of a binomial distribution, valid when n_T is greater than 100 and p is smaller than 0.01 (*15*).

Equation 3 has important ramifications. The analysis of microvolumes of very dilute solutions is ultimately limited, not by instrument sensitivity but by statistical errors in sampling. For example, if 1% relative standard deviation is desired for sampling a homogeneous solution that is 10^{-8} M in analyte, a sample volume of no less than 2 pL is required.

The impact of statistical sampling errors in detecting a very dilute analyte in solution is now examined. We choose fluorescence as an example technology because it has good potential for single molecule detection in solution and is well suited to miniaturization. Much of the discussion that follows could be modified for other detection schemes.

As smaller volumes of solution are probed, diffusion times through the sample observation (probe) volume will be reduced. At some point, a plot of signal vs. time will have an additional noise component due to the sampling uncertainty. This occurs because diffusion replaces one "sample" with another. This effect will also be observed in flowing streams.

Dovichi et al. made a distinction between the volume "sampled" by the detector and the probe volume (*3*). This convention will be used here. Thus, the probe volume is the

0003-2700/86/0358-2567$01.50/0 © 1986 American Chemical Society